

VI-C Generation of Ultrashort Optical Pulse for Time-Resolved Spectroscopy

It is important to improve time-resolution of time-resolved spectroscopy because higher time-resolution gives us a chance to observe new "fast" phenomena that can not be recognized with lower time-resolution. Nowadays, we can generate sub-10 fs pulses using modern laser technology. Although it is not easy task to handle such short optical pulses and to employ them for the study in molecular science, time-resolved spectroscopy utilizing such pulses are very important and desirable. We constructed two optical setups to generate ultrashort optical pulses whose duration is in the range from ten to a few tens of femtoseconds.

VI-C-1 Development of UV-Excited Transient Absorption Spectrometer Based on 10-fs Pulses

TAKEUCHI, Satoshi; TAHARA, Tahei

Ultrashort optical pulses have been widely used in time-resolved spectroscopic studies of the excited state properties and the reaction dynamics of molecules. The time-resolution in most of these studies, however, has been so far limited to the range of 200–500 fs. Particularly in experiments using ultraviolet pulses, the time-resolution tends to become worse due to broadening of the pulse duration in the frequency conversion process to the ultraviolet. In this project trying to achieve better time-resolution in molecular spectroscopy, we have constructed a high-power optical parametric amplifier (OPA) producing 10-fs pulses in the visible region, and utilized it for the transient absorption measurements (Figure 1). In the OPA, a femtosecond white-continuum seed pulse is amplified twice in a BBO nonlinear crystal, which is pumped by the second harmonic (400 nm) of the amplified Ti:sapphire laser pulse. The output pulse is then sent to a double-pass prism compressor to correct its phase dispersion. The autocorrelation of the compressed pulse (Figure 2A) indicates that the pulse duration is as short as 9.6 fs. The OPA is tunable in the wavelength region of 500–750 nm, and the typical pulse energy is 10–15 μJ at a 1 kHz repetition rate. Next, in the transient absorption spectrometer, most of the 10-fs pulse energy from the OPA is focused into a thin BBO crystal to generate the second harmonic tunable in the near-ultraviolet (250–375 nm). After the phase-dispersion compensation with a prism pair, the second harmonic is used as a pump pulse for photoexcitation of the sample. The minor rest of the 10-fs pulse is used as a probe and a reference pulse. The time-resolution of this spectrometer is evaluated as 35 fs from a cross-correlation trace between the pump and probe pulses (Figure 2B). This value is an order of magnitude better than that of a conventional transient absorption spectrometer using femtosecond white-continuum pulses. Observation of the excited state dynamics in a very early time region is now in progress by using this spectrometer.

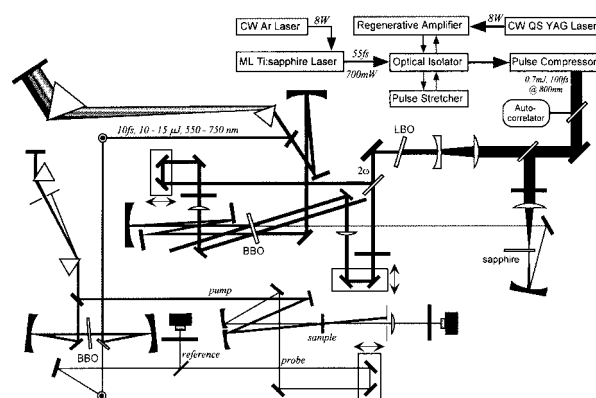


Figure 1. Experimental setup for uv-excited transient absorption measurements using 10-fs pulses.

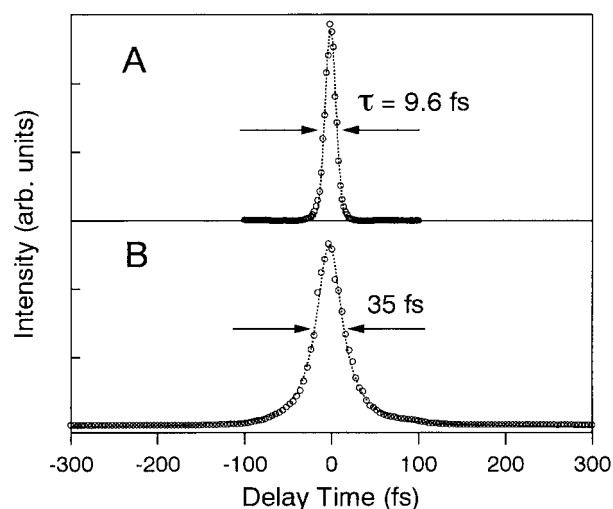


Figure 2. Autocorrelation of the OPA output pulse (A), and cross-correlation trace between the pump and probe pulses used in the transient absorption spectrometer (B).

VI-C-2 Generation of Ultra-Short Pulses Using a Krypton Gas-Filled Hollow Fiber

FUJIYOSHI, Satoru; TAKEUCHI, Satoshi; TAHARA, Tahei

We have constructed an apparatus to generate ultrashort pulses using a krypton gas-filled hollow fiber.¹⁾ This apparatus consists of two parts. In the first part, the femtosecond pulse from a Ti:sapphire regenerative amplifier (100 fs, 800 nm, 210 μJ , 1 kHz) is coupled into a hollow fiber that is filled with krypton gas. The input pulse spectrum becomes broader due to the self phase modulation in the gas while the pulse passes

through the fiber. The spectrum of the input pulse and that of the output pulse from the hollow fiber are shown in Figure 1a. Spectral width of the input pulse is 12 nm (FWHM) and that of the output pulse covers a wide range from 770 to 870 nm. In the second part, the broadened output pulse is sent to a prism compressor to correct its group velocity dispersion. Autocorrelation of the final compressed pulse is shown in Figure 1b. The pulse duration is as short as 30 fs as well as pulse energy of 5 μ J has been obtained.

Reference

1) M. Nisoli *et al.*, *Opt. Lett.* **22**, 522 (1997).

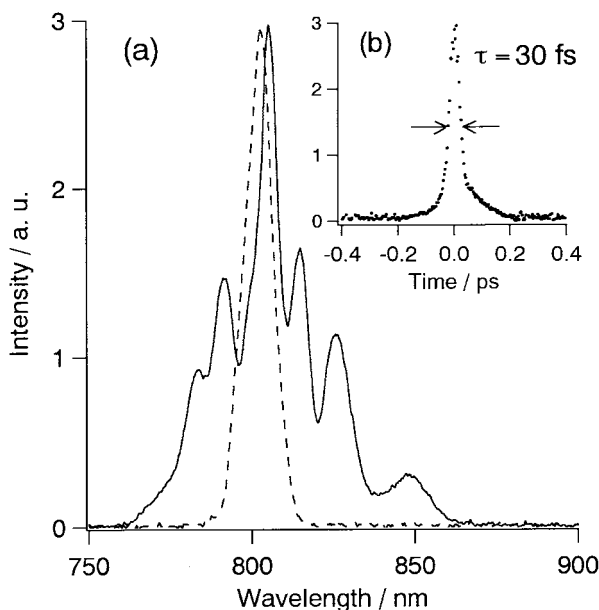


Figure 1. (a) Spectra of input pulse (dashed line) and output pulse (solid line) of hollow fiber. (b) Auto-correlation trace. The pulse duration (FWHM) is 30 fs.

VI-D Studies of Primary Photochemical/Physical Processes Using Femtosecond Fluorescence and Absorption Spectroscopy

Ultrafast spectroscopy is playing an essential role in elucidation of photochemical reactions. Thanks to the recent advance in laser technology, we are now able to observe the dynamics of chemical reactions taking place in the femtosecond time region. In this project, we are studying primary photochemical/physical processes in the condensed phase using time-resolved fluorescence and absorption spectroscopy with a few hundreds femtoseconds time-resolution. Time-resolved fluorescence and absorption spectroscopy are complimentary to each other. The advantage of fluorescence spectroscopy lies in the fact that fluorescence originates from the transition between the “well-known” ground state and the excited state in question. Thus time-resolved fluorescence spectroscopy can afford unique information not only about the dynamics but also other properties of the excited singlet states such as their energies and oscillator strengths. On the other hand, however, time-resolved absorption spectroscopy is considered to be more versatile because it can detect not only fluorescent excited singlet states but also other “dark” transients. In this year, we investigated the ultrafast proton transfer reaction and the relaxation process of the highly excited states of several fundamental molecules, with use of these time-resolved electronic spectroscopy.

VI-D-1 Vibronic Relaxation of Polyatomic Molecule in Non-polar Solvent: Femtosecond Anisotropy/Intensity Measurements of the S_n and S_1 Fluorescence of Tetracene

SARKAR, Nilmoni; TAKEUCHI, Satoshi; TAHARA, Tahei

[*J. Phys. Chem. A* **103**, 4808 (1999)]

The electronic and vibrational relaxation of tetracene have been studied in solution by femtosecond time-resolved fluorescence spectroscopy. Tetracene was initially photoexcited to the highly excited singlet (S_n) state, 1B_b , and the dynamics of the fluorescence from the 1B_b state and the 1L_a state (S_1) were investigated by fluorescence up-conversion. The fluorescence from the 1B_b state was observed in the ultraviolet region, and its lifetime was determined as ~ 120 fs. The anisotropy of

the 1B_b fluorescence was close to 0.4, which assured that the fluorescence is emitted from the excited state that was prepared by photoexcitation. The visible fluorescence from the 1L_a state showed a finite rise that agreed well with the decay of the 1B_b fluorescence (Figure 1A). Negative anisotropy was observed for the 1L_a fluorescence, reflecting that the 1L_a transition moment is parallel to the short axis of the molecule and hence perpendicular to the 1B_b transition moment. The anisotropy of the 1L_a fluorescence, however, showed a very characteristic temporal behavior in the femtosecond time region: it exhibited a very rapid change and reached a certain value that is deviated from -0.2 (Figure 1B). The anisotropy data indicate that the 1L_a fluorescence contains not only short-axis polarized component but also long-axis polarized component and that the ratio between the two components depends on both time and wavelength. The long-axis polarized component in the 1L_a fluorescence was assigned to the

1B_b -type fluorescence that appears as the result of the vibronic coupling between the 1L_a state and the 1B_b state. The observed initial rapid change of the anisotropy suggests that the highly excited vibrational states in the 1L_a state which are strongly coupled with the 1B_b state are first populated preferentially when the molecule is relaxed from the 1B_b state to the 1L_a state. The visible fluorescence anisotropy vanishes gradually due to the rotational diffusion in a few tens of picoseconds. In the picosecond region, we also observed additional dynamics in the fluorescence intensity whose time constant was about 12 ps. This dynamics was assigned to the vibrational relaxation (cooling) in the 1L_a state. The observed relaxation processes that take place after photoexcitation of tetracene are sketched in Figure 2.

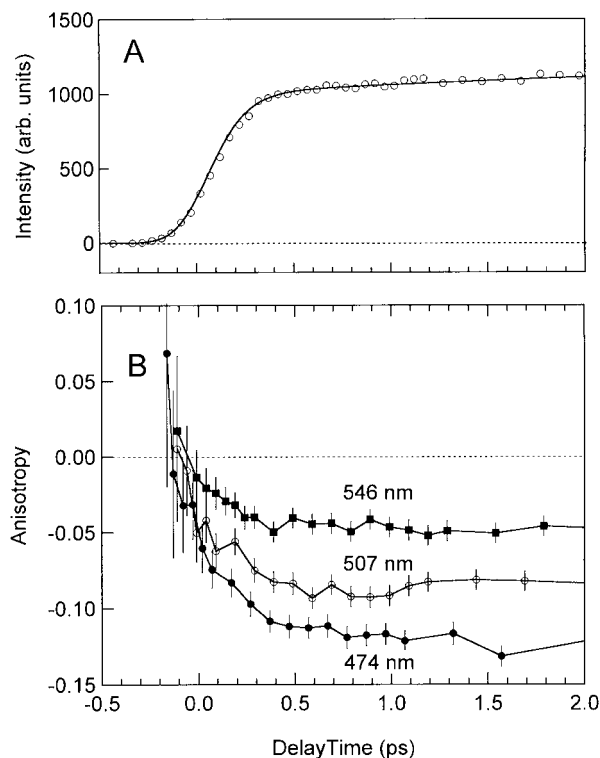


Figure 1. Early-time dynamics of the fluorescence intensity and anisotropy obtained from tetracene in hexadecane (273 nm excitation). (A) Time-resolved fluorescence signal at 507 nm measured with the magic angle condition. (B) Time-resolved fluorescence anisotropy measured at three different wavelengths (474, 507 and 546 nm).

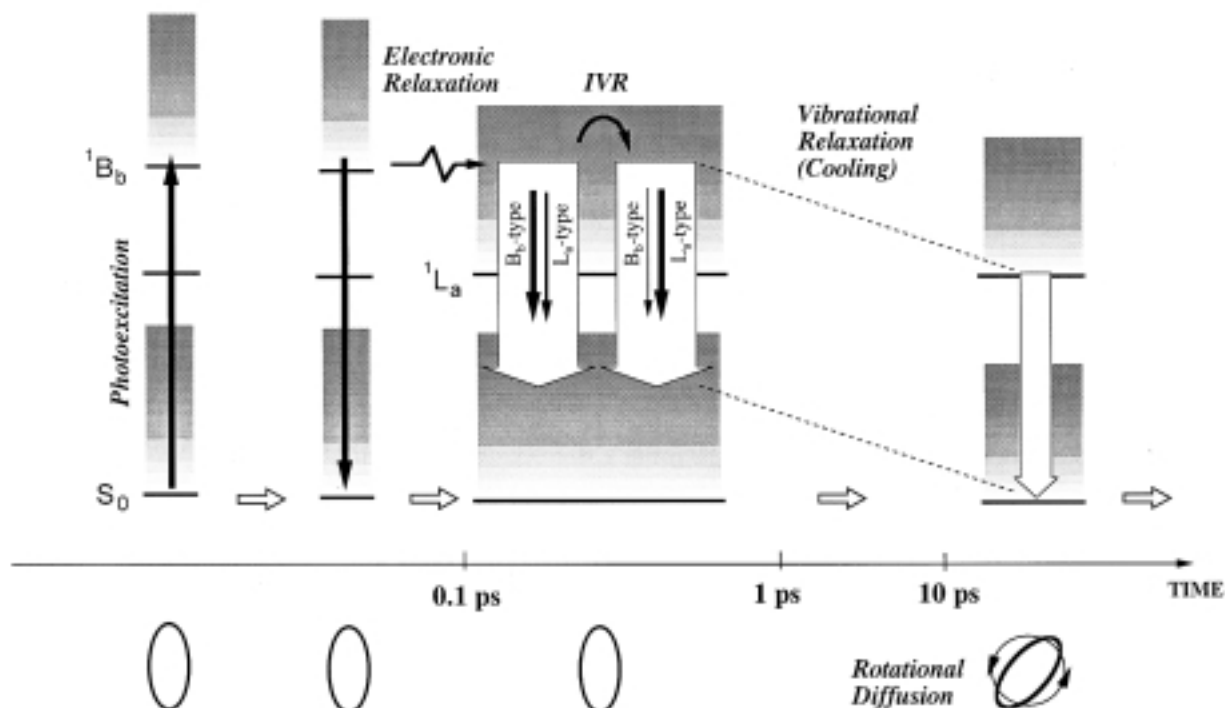


Figure 2. Schematic diagram depicting the relaxation processes of tetracene in solution following the direct photoexcitation to the highly excited singlet (S_1) state.

VI-D-2 Determination of the Excited-State Transition-Moment Directions of 7-Azaindole Dimer by Femtosecond Fluorescence Anisotropy Measurements

TAKEUCHI, Satoshi; TAHARA, Tahei

Time-resolved fluorescence anisotropy data can afford much information not only about the orientational diffusion of molecules in solution but also about the transition moment of the fluorescing state. In fact, the anisotropy change observed in the femtosecond time region does not arise from the orientational diffusion but is mainly caused by changes in the transition-moment direction, because the molecular motion is almost neglected in this short time region. Femtosecond fluorescence anisotropy measurement is, therefore, a powerful method which enables us to determine the transition-moment directions. In order to know the transition-moment directions of the three excited states (dimer L_b , dimer L_a , and tautomer L_a) which appear successively in the proton transfer reaction of 7-azaindole dimer, we measured fluorescence anisotropy of this dimer at three visible wavelengths with a 230-fs time-resolution (Figure 1). The anisotropy shows a rapid decay within one picosecond, and its feature depends on the observation wavelength. An additional slow component (12 ps) observed in every wavelength is due to the orientational diffusion of the dimer. We have simulated the time-dependence of the anisotropy on the basis of a model that includes the three excited states, and determined relative angles of the transition moments of each excited state by a fitting procedure (dotted curves). It was found that the wavelength dependence of the observed anisotropy can be explained by spectral difference of the fluorescences from the three excited states and that relative angle obtained from the data taken at the three wavelengths agreed very well with one another. We concluded that the relative transition-moment directions of the dimer L_a and tautomer L_a states with respect to the initially-populated dimer L_b state are 39° and 42° , respectively. It was reported by a rotational contour analysis of 7-azaindole in gas phase that the transition moment of the L_b state is 16° tilted from the inertial axis. Consequently, we can finally determine the absolute direction of the transition moments with respect to the inertial axis as 16° , 55° , and 58° for the dimer L_b , dimer L_a , and tautomer L_a states, respectively.

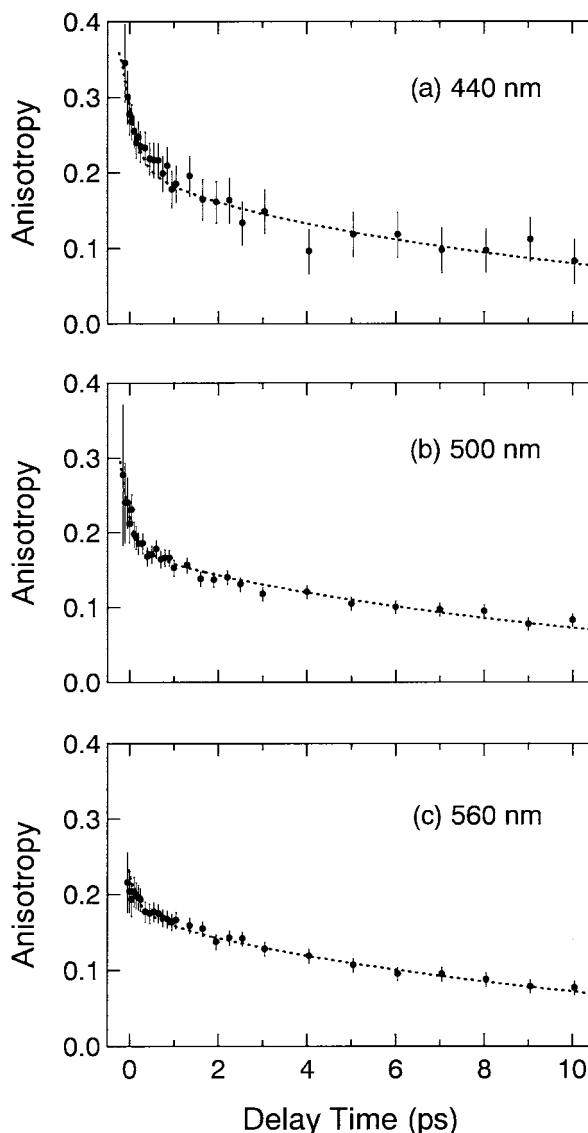


Figure 1. Time-resolved fluorescence anisotropy of 7-azaindole dimer in hexane measured at 440 (a), 500 (b), and 560 nm (c). Calculated anisotropy is also shown by a dotted curve.

VI-D-3 Investigation of Excited State Intramolecular Proton Transfer in Anthralin by Femtosecond Time-Resolved Fluorescence Spectroscopy

ARZHANTSEV, Sergei; TAKEUCHI, Satoshi; TAHARA, Tahei

Numerous elementary photoreactions in condensed phase occur on ultrafast time scale and femtosecond spectroscopy provides direct insight into the dynamics of such processes. The photoinduced intramolecular proton transfer of hydrogen-bonded molecules is a topic of current interest. Anthralin (1,8-dihydroxy-9(10H)-anthracenone) is of biological and pharmacological importance as antipsoriatic drug. Steady-state fluorescence excitation and emission spectra display an unusually large Stokes shift, indicating intramolecular proton transfer. The proposed scheme of photoinduced reaction is shown in Figure 1. Time-resolved fluorescence measurements were performed in a wide spectral

region from 480 nm to 690 nm. Several time-resolved fluorescence traces are presented in Figure 2. We observed the fast decays in blue side and coinciding fast rises in red side of the spectrum in (sub)picosecond time region, which gave us the information about the proton transfer rate. The global fit procedure was applied for quantitative analysis of experimental data. As results of fitting procedure, characteristic time constants ($\tau_1 = 0.1$ ps, $\tau_2 = 1.4$ ps, $\tau_3 = 120$ ps) of excited state dynamics were obtained. The excited state dynamics were discussed in terms of excited-state intramolecular proton transfer and other pathways of the energy relaxation.

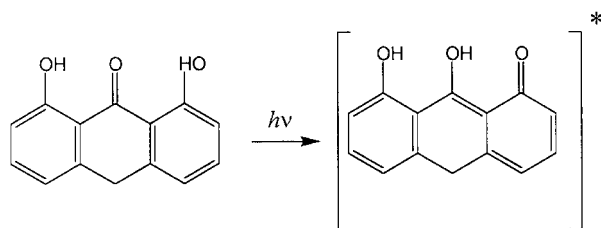


Figure 1. The proposed scheme of proton transfer in anthralin.

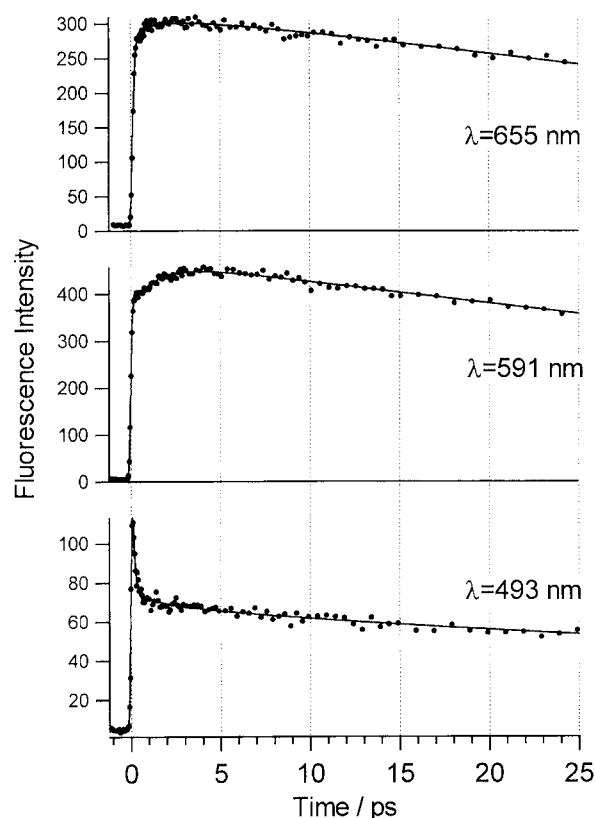


Figure 2. Time-resolved fluorescence traces obtained from anthralin at 655, 591 and 493 nm. The dots are experimental data and the solid curves are the results of the fitting analysis.

VI-D-4 Relaxation Kinetics of the S_n and S_1 States of Biphenyl Probed by Femtosecond Fluorescence Anisotropy

IWATA, Koichi¹; TAKEUCHI, Satoshi; TAHARA, Tahei
(¹Univ. Tokyo)

Fluorescence intensity and its anisotropy decay of biphenyl were measured in hexane solution. The sample solution was photoexcited with a linearly polarized femtosecond light pulse at 270 nm. Time dependence of the fluorescence intensity as well as its anisotropy was measured with the up-conversion method. The observed fluorescence decay curve showed a fast decay component of 0.4 ps, in addition to a slow component corresponding to the reported fluorescence decay of 16 ns. The observed fluorescence anisotropy value at time 0 was approximately 0.4, indicating that the direction of the fluorescence transition dipole at time 0 is same as the S_n - S_0 absorption at 270 nm. The observed anisotropy change was well fitted by a double exponential decay function, with time constants of 0.2 ps and 9 ps. The fast component represents the S_n - S_1 internal conversion process, while the slow component corresponds to the rotational diffusion of the S_1 state. From the extrapolated value of the slow component at time 0, the angle between the effective transition dipoles of the S_n - S_0 transition and the S_1 - S_0 transition was estimated to be 27 degrees.

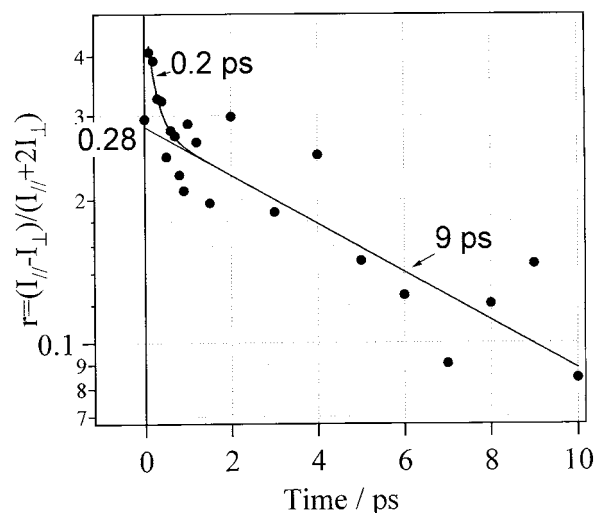


Figure 1. Time dependence of femtosecond fluorescence anisotropy of biphenyl.

VI-D-5 Lifetime Measurements of S_2 Emission from Zinc(II) Porphyrins by the Femtosecond Up-Conversion Method

ASANO-SOMEDA, Motoko¹; ARZHANTSEV, Sergei; TAHARA, Tahei
(¹Tokyo Inst. Tech.)

In violation of Kasha's rule, upper excited-state emission has been observed for some polyatomic molecules. For instance, a variety of diamagnetic metalloporphyrins exhibit fluorescence from the secondary excited singlet (S_2) state even under the steady-state condition. Relatively intense S_2 emission of metalloporphyrins must be related with their characteristic electronic structure. In the typical diamagnetic metalloporphyrins, the S_1 and S_2 states are described as a 50-50 admixture of two common (π, π^*) configurations, and this leads to almost parallel surfaces in the S_1 and S_2 states. In addition, there is a reasonably

large energy gap between the S_1 and S_2 states. Such features of metalloporphyrins slow $S_2 \rightarrow S_1$ internal conversion rates, thus allowing observation of S_2 emission.

Zinc(II) porphyrin is one of the typical diamagnetic metalloporphyrins and exhibits S_2 fluorescence. While subpicosecond lifetimes are estimated for such porphyrins from the quantum yields of S_2 emission, it is crucial to determine the lifetimes by means of time-resolved measurements. We have applied the femto-second up-conversion method to a series of zinc(II) porphyrins. Figure 1 shows the decay of S_2 and rise of S_1 emission signals of TMPZn(II) (TMP denotes tetramethylporphyrin) measured with 400 nm excitation. Both kinetic traces give the same time constant of 1.6 ps, which corresponds to the S_2 lifetime.

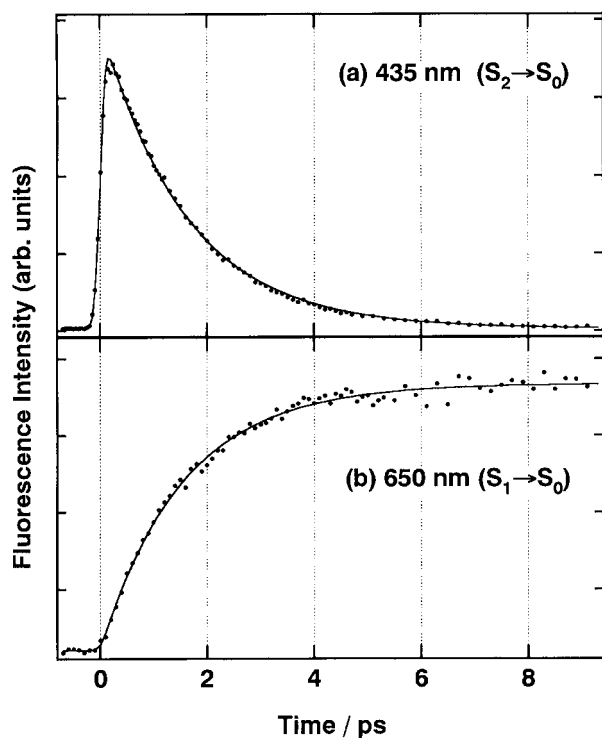


Figure 1. (a) Decay of S_2 and (b) rise of S_1 emission signals of TMPZn in toluene upon femtosecond laser irradiation at 400 nm. Experimental results are given by dots along with the best fitting curves in solid lines.

VI-D-6 Femtosecond Absorption Study on Ultrafast Decay Dynamics of Photoexcited Cu(II)(TMpy-P4) in Water Solvent

JEOUNG, Sae Chae; TAKEUCHI, Satoshi; TAHARA, Tahei; KIM, Dongho¹
(¹KRISS)

[*Chem. Phys. Lett.* **309**, 369 (1999)]

Femtosecond time-resolved absorption spectroscopy was employed to investigate the relaxation dynamics of photoexcited copper(II) tetrakis(4-N-methylpyridyl)porphyrin (Cu(II)(TMpy-P4)) in neat water. It was found that the transient absorption spectra as well as their temporal profiles exhibit a strong pump-power dependency, which is probably the cause of the

discrepancy in the previous reports about dynamics of this molecule. It was concluded that the multiphoton ionization of solvent water takes place under the high pump-power condition. Time-resolved absorption spectra of Cu(II)(TMpy-P4) were measured with the pump power as low as 0.03 mJ/cm^2 , and it was confirmed that the relaxation process finishes within 100 ps. We observed temporal changes of the excited-state(s) absorption in the picosecond region as well as the double exponential recovery of the ground state bleaching. The obtained time-resolved absorption data revealed that the relaxation process of photoexcited Cu(II)(TMpy-P4) in water is rather complicated and they suggested that several transient species (excited states) appear in the course of the relaxation. The relaxation mechanism of photoexcited Cu(II)(TMpy-P4) as well as the interaction with solvent water was discussed.

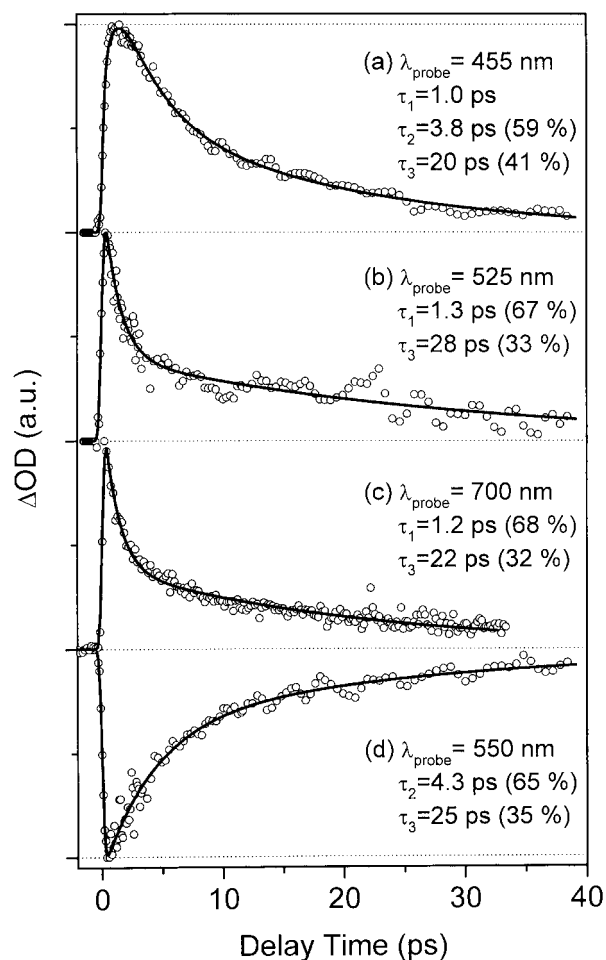


Figure 1. The time-resolved absorption changes of photoexcited Cu(II)(TMpy-P4) in water at three wavelengths of 455 (a), 525 (b) and 700 nm (c). The temporal change of the Q-band bleaching at 550 nm (d) was determined after correcting the baseline variation due to the photoinduced absorption.

VI-E Studies of Photochemical Reactions Using Picosecond Time-Resolved Vibrational Spectroscopy

Time-resolved vibrational spectroscopy is a very powerful tool for the study of chemical reactions. It often affords detailed information about the molecular structure of short-lived intermediates, which is not obtainable with time-resolved electronic spectroscopy. However, for molecules in the condensed phase, we need energy resolution as high as 10 cm^{-1} in order to obtain well-resolved vibrational spectra. This energy resolution is compatible only with time-resolution slower than picosecond because of the limitation of the uncertainty principle. In this sense, picosecond measurements are the best compromise between energy resolution and time resolution for time-resolved frequency-domain vibrational spectroscopy. In this project, we study photochemical processes and short-lived transient species by using picosecond time-resolved Raman spectroscopy. In this year, we focused on trans-azobenzene that is a prototypical molecule showing fast cis-trans isomerization. We studied the electronic and vibrational relaxation processes as well as the structure of the S_1 state of this molecule. In addition, while doing time-resolved Raman work, we recently noticed that amplified picosecond pulses are suitable for the excitation of hyper-Raman scattering.

VI-E-1 Picosecond Time-Resolved Raman Study of Trans-Azobenzene

FUJINO, Tatsuya; TAHARA, Tahei

[*J. Phys. Chem. A* in press]

The electronic and vibrational relaxation of photoexcited trans-azobenzene were investigated by picosecond time-resolved Raman spectroscopy. The second and third harmonic pulses of the regeneratively amplified output of a Ti:sapphire laser were used as the probe (410 nm) and the pump (273 nm). The frequency resolution of the measurement was approximately 10 cm^{-1} and time resolution was about 2 ps. With the 273-nm pumping pulse, the molecule is initially excited to the $S_2(\pi\pi^*)$ state, and the 410-nm probing wavelength is in resonance with the $S_n \leftarrow S_1$ transient absorption that appears in accordance with the decay of the S_2 state. Several transient Raman bands assignable to the S_1 state were observed immediately after photoexcitation. The lifetime of the S_1 state showed a significant solvent dependence and it was determined as $\sim 12.5\text{ ps}$ in ethylene glycol and $\sim 1\text{ ps}$ in hexane. Time-resolved anti-Stokes Raman measurements were also carried out for hexane solution to obtain information about vibrational relaxation process (Figure 1). We observed almost all S_1 Raman band in the anti-Stokes spectra, which implies that the S_1 state is highly vibrationally excited. In addition, several anti-Stokes Raman bands due to the S_0 state were observed after the decay of the S_1 state, indicating that the vibrationally excited S_0 azobenzene was generated after electronic relaxation in hexane. The lifetime of vibrationally excited S_0 azobenzene was evaluated as $\sim 16\text{ ps}$ by the analysis for the intensity change of the anti-Stokes NN stretching band. The relaxation process of photoexcited *trans*-azobenzene clarified in the present study is depicted in Figure 2.

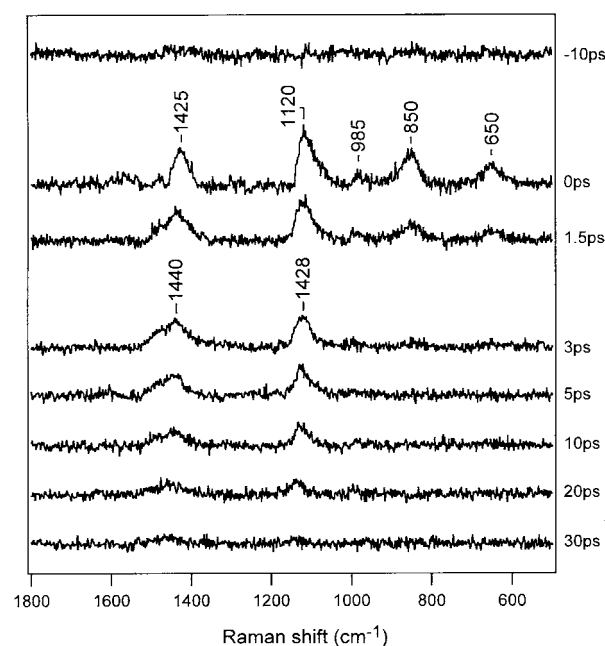


Figure 1. Picosecond time-resolved anti-Stokes Raman spectra of azobenzene in hexane in the delay time range from -10 ps to 30 ps ($1.5 \times 10^{-2}\text{ mol dm}^{-3}$; pump at 273 nm; probe at 410 nm).

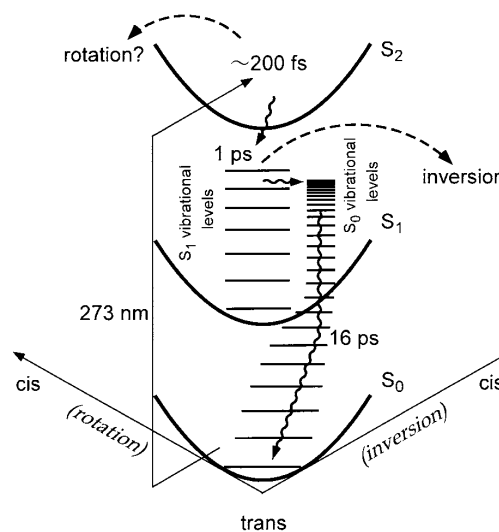


Figure 2. The relaxation mechanism of photoexcited *trans*-azobenzene (in hexane).

VI-E-2 Molecular Structure of S_1 Azobenzene: Vibrational Frequency of the NN Stretch Mode in the S_1 and S_0 State

FUJINO, Tatsuya; TAHARA, Tahei

Time-resolved vibrational spectra contain much information about the molecular structure of transient species. Concerning the S_1 state of azobenzene, information about the structure around the central NN bond is the most important because it can afford a clue to understand how the S_1 state participates in the photoisomerization process. In this sense, the assignment of the NN stretching vibration is crucial. We synthesized a ^{15}N -substituted analogue and measured S_1 Raman spectra in order to make unambiguous assignment about this key vibration and to discuss the molecular structure of the S_1 state.

Figure 1 shows transient Raman spectra of the normal species and the ^{15}N analogue ($(\text{C}_6\text{H}_6^{15}\text{N})_2$) of the S_1 state of azobenzene. The spectra were measured for ethylene glycol solutions. The Raman spectra of the S_0 state are also shown in this figure for the comparison. In the S_1 spectra, it is clearly recognized that the Raman band at 1428 cm^{-1} shows a 27-cm^{-1} downshift with ^{15}N substitution. This S_1 band is straightforwardly attributable to the NN stretching vibration in the S_1 state. The NN stretching frequency in the S_1 state is almost same as that in the S_0 state (1440 cm^{-1}), which manifests that the NN bond in S_1 azobenzene retains a double bond character. The double bond nature of the NN bonding as well as high similarity in the spectral feature between S_1 Raman and S_0 Raman suggests that the observed S_1 azobenzene has a planar structure around the central NN bond.

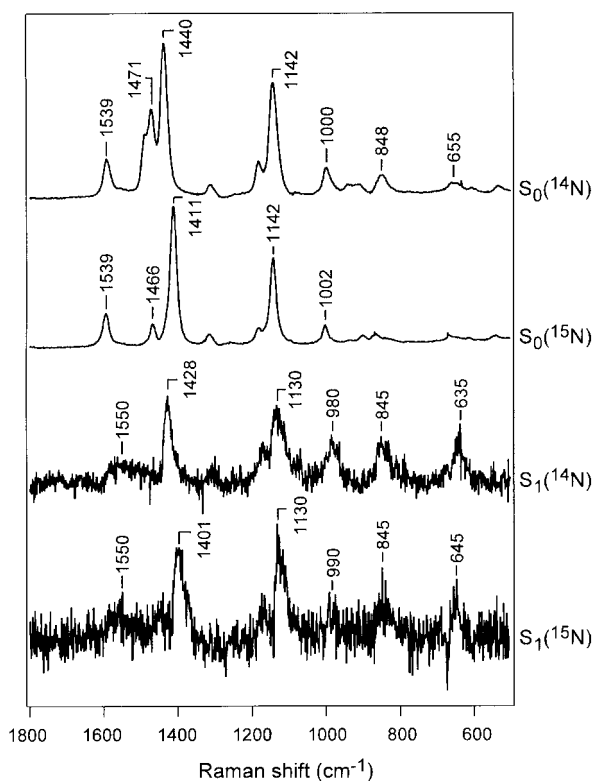


Figure 1. Raman spectra of azobenzene in the S_1 state and the S_0 state (in ethylene glycol). From the top to the bottom, normal species in the S_0 state, ^{15}N analogue in the S_0 state, normal species in the S_1 state, and ^{15}N analogue in the S_1 state. The S_1 spectra were taken at 0 ps. ($1.5 \times 10^{-2}\text{ mol dm}^{-3}$; pump at 273 nm; probe at 410 nm).

VI-E-3 Observation of Resonance Hyper-Raman Scattering of *all-trans* Retinal

MIZUNO, Misao; TAHARA, Tahei; HAMAGUCHI, Hiro-o¹
(¹Univ. Tokyo)

High peak powered ultrafast lasers allow us to observe a variety of higher order optical processes. We recently found that a fairly strong hyper-Raman scattering of *all-trans* retinal can be observed by using the excitation with amplified picosecond pulses under a resonance condition, even from a diluted solution. A typical resonance hyper-Raman spectrum excited at 800 nm (ω) is shown in Figure 1(a). The probe pulse was the output of the picosecond regenerative amplifier of a Ti:sapphire laser system. The pulse width and the pulse energy were about 2 ps and 10 μJ , respectively. The resonance Raman spectrum excited at 400 nm (2ω) is shown in Figure 1(b), for comparison. The spectral pattern of the hyper-Raman and the Raman spectra is very similar to each other, although the intensity enhancement arises from two-photon resonance in hyper-Raman process while it is due to one-photon resonance in ordinary Raman. The similarity of these spectra suggests that resonance mechanism of hyper-Raman scattering is attributed to the A-term of the resonance hyper-Raman theory.¹⁾ We also measured resonance hyper-Raman spectra of *all-trans* retinal by probing at every 10 nm from 770 nm to 840 nm, and examined the excitation profiles.

Reference

- 1) Y. C. Chung and L. D. Ziegler, *J. Chem. Phys.* **88**, 7287 (1988).

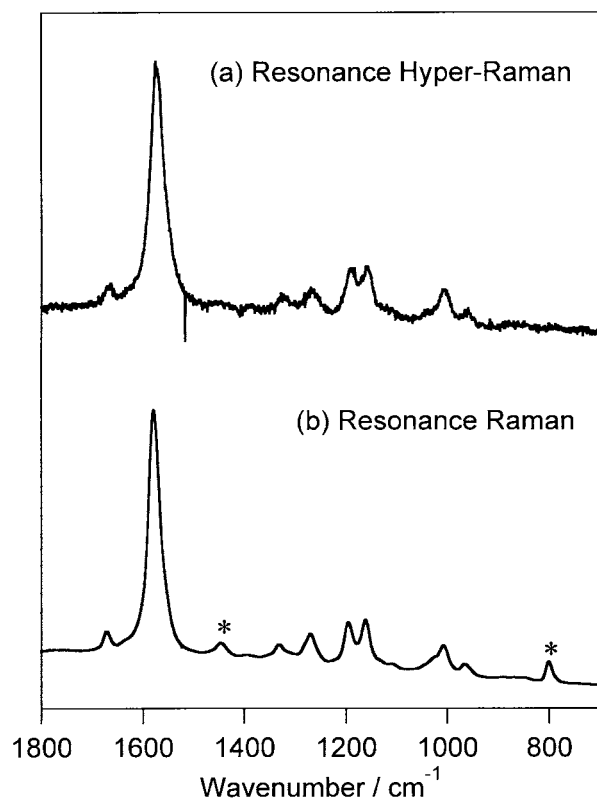


Figure 1. Comparison of (a) resonance hyper-Raman and (b) resonance Raman spectra of all-trans retinal in cyclohexane (1×10^{-3} mol dm⁻³). Excitation wavelength is 800 nm for resonance hyper-Raman, and 400 nm for resonance Raman. The asterisks (*) indicate solvent bands.